Global J. Environ. Sci. Manage. 10(1): 1-20, Winter 2024, Serial #37

Global Journal of Environmental Science and Management
(GJESM)

Homepage: https://www.gjesm.net/

Podcasts

ORIGINAL RESEARCH PAPER

# Exploring the upper ocean characteristics of a bay using coastal and regional ocean community model

**D. Jaishree*, P.T. Ravichandran**

*Department of Civil Engineering, Faculty of Engineering and Technology, SRM Institute of Science and Technology, Kattankulathur - 603203, Chengalpattu District, Tamil Nadu, India*

**ARTICLE INFO**

***Article History:***
Received 25 February 2023
Revised 04 June 2023
Accepted 10 July 2023

***Keywords:***
Bay of Bengal (BoB)
Coastal and Regional Ocean COmmunity model (CROCO)
Numerical model
Reanalysis data
Salinity and Temperature

**ABSTRACT**

**BACKGROUND AND OBJECTIVES:** The innovativeness of this study lies in achieving a comprehensive understanding of the seasonal variations and oceanic characteristics of the Bay of Bengal by addressing the complex interplay of large-scale ocean-atmosphere dynamics. The study aimed to understand the upper ocean characteristics of the Bay of Bengal by analyzing the surface variables such as salinity and temperature using a high-resolution model simulation. To accomplish this, advanced high-resolution numerical simulations were employed, utilizing the coastal and regional ocean community model. This model was crucial for investigating and analyzing the circulation features throughout the entire Bay of Bengal, contributing knowledge and insights about the coastal and regional oceanographic community.
**METHODS:** To investigate the temporal variability of the upper ocean in the Bay of Bengal, climatological simulations were performed over eight years using the coastal and regional ocean community model. Including a three-year spin-up phase facilitated the adjustment of the model to initial conditions and the attainment of equilibrium, ensuring its fidelity to real-world conditions. The follow-up analyses and comparisons were performed five years after the spin-up phase. The primary objective of this study was to examine the temporal evolution of the kinetic energy throughout the eight-year simulation. The volume-averaged kinetic energy was computed, revealing a gradual increase throughout the simulation, with particularly pronounced enhancements observed during the monsoon period. A Taylor diagram was used for predicting the model with the other data sets.
**FINDINGS:** The analysis is performed above the surface and sub-surface oceanic layers with prominent dynamics. The temperature and salinity for the surface and sub-surface layers were validated and analyzed for their seasonal variations. The simulations were validated against the existing satellite, reanalysis, and in situ data.
**CONCLUSION:** The innovativeness of this study lies in its successful demonstration of the seasonal variability of temperature and salinity in the Bay of Bengal. Through extensive validations, it establishes the model to accurately simulate the climatological surface features of the Bay of Bengal. This study highlights the effectiveness of numerical models when combined with observations, and the data were reanalyzed, showcasing their utility as valuable tools for studying oceanic conditions. The utilization of a Taylor diagram further supports the validation and excellent performance of the model compared to other available datasets. During the simulation, there is a high correlation (0.96) between the evolution of the salinity and temperature values obtained from the model and the corresponding data from the World Ocean Atlas. This indicates a strong agreement between the model-based simulations and the assimilated data, as supported by the notable correlation values of 0.96 for salinity and temperature. These findings reinforce the existing knowledge regarding the influential role of monsoon winds in shaping the circulation patterns within the Bay of Bengal. Overall, this study contributes to advancing our understanding of the ocean dynamics of the region and underscores the importance of considering seasonal variations for comprehensive oceanographic research, coastal management, climate modeling, and future studies in the Bay of Bengal.

DOI: 10.22035/gjesm.2024.01.***



| NUMBER OF REFERENCES | NUMBER OF FIGURES | NUMBER OF TABLES |
|---|---|---|
| 44 | 11 | 2 |

*Corresponding Author:
Email: *jaishred@srmist.edu.in*
Phone: +900 3180 202
ORCID: 0000-0003-0401-068X

Note: Discussion period for this manuscript open until April 1, 2024 on GJESM website at the "Show Article".

## INTRODUCTION

The Bay of Bengal (BoB) is a massive body of water situated at the northeastern edge of the Indian Ocean, bordered by the Indian subcontinent and Southeast Asia. (Rao *et al*., 2011; Masumoto *et al*., 2005). It spans an approximately 2.2 million $km^2$ area, with its deepest point reaching around 5,000 m, and is surrounded by some of the most populated regions on Earth. (Schott *et al.,* 2009; Schott and McCreary, 2001). The BoB is an important shipping lane and fishing ground, and it plays a major role in the formation of monsoon rains in the region. (Webster *et al.,* 1998). The BoB experiences a monsoon-dominated climate characterized by clearly distinguishable wet and dry seasons. (Jourdain *et al*., 2013; Liebmann *et al*., 1994; Maneesha *et al*., 2012). During the monsoon season (June – September), the region experiences heavy rainfall and strong winds due to the southwesterly flow of moist air. In the winter months (December – February), the BoB experiences dry and cool weather with winds blowing from the northeast (Roy Chowdhury *et al*., 2021). Tropical cyclones and storm surges, particularly during the peak pre- and post-monsoon season, are also experienced in the Bay. (Anandh *et al*., 2018). Oceanographers worldwide have been captivated by the unique dynamics of the BoB, which can be attributed to its geographic location, with a landlocked northern limit causing an alternation in the monsoon winds and seasons. (Akhter *et al*., 2021: Vinayachandran *et al.,* 1996). The seasonal monsoon precipitation has an impact on the agricultural activity in the neighboring nations as well. Through the advancement of numerical simulation tools, the comprehension of the impact of various physical parameters, such as temperature and salinity as the main parameters, and other parameters like tidal forcing, Rossby and Kelvin waves, along with the wind stress curl have on the ocean circulations has been greatly enhanced. (Sil and Chakraborty., 2012). The BoB is also susceptible to various natural hazards, including tropical cyclones, storm surges, and tsunamis, which cause significant damage and loss of life. As a result, BoB is the focus of extensive research in oceanography, meteorology, geology, disaster risk reduction, and management. In addition, the BoB is strategically important to several regional countries, particularly in maritime trade and security. Additionally, the BoB is a prominent region for energy exploration and production, harboring substantial oil and gas reserves in its offshore territories. In the BoB, the predominantly warm conditions are one of the foremost reasons for forming seasonal cyclones (Ts *et al*., 2020). Given the potential scope for the formation of depressions and the intensification of cyclones in the BoB, it becomes crucial to comprehensively understand the intricate interactions among the oceans and atmosphere within the bay. The oceans of the world, mainly the uppermost 700 m, are presently undergoing a warming trend (Levitus *et al*., 2012) as the oceans are absorbing more amounts of energy that can result in an intensification of the air-sea interactions occurring over the world (Collins *et al*., 2010). To study the influence of atmosphere-ocean interactions on the variations in temperature and salinity, mixed layer depth (MLD), and circulations in the BoB and the Arabian Sea, a multitude of observational and modeling-based studies have been undertaken. (Gao *et al*., 2014) These studies aim to better understand these key oceanographic parameters in the area. (Amsalia *et al*., 2022; Dyn 2010; Akhil *et al*., 2014; Mahadevan *et al*., 2016). The part of the Western Bay exhibits various oceanic features, such as the East India Coastal Current (EICC) and the Western Boundary Current (WBC) discontinuities, inconsistency in the boundary current, and a disrupted summer monsoonal boundary current. The BoB contributes markedly to regional climate variability, particularly regarding air-sea exchanges, in a significant manner. (Das *et al*., 2019; Dey *et al*., 2017). The BoB has a tropical climate characterized by high sea surface temperatures (SST) ranging from 27 – 30 °C and high sea surface salinity (SSS) levels of around 35 – 37 practical salinity units (psu). The SST and SSS in the BoB vary during the monsoon season and are influenced by the freshwater influx from major rivers like the Ganga and Brahmaputra (Rao and Behera, 2005). In conjunction with the Arabian Sea and the northern Bay, the SSS displays opposite behavior in response to the varying environmental forces. The salinity decreases in the absence of wind and shortwave radiation forces, whereas it increases in the absence of freshwater flux forces. (Srivastava *et al*., 2018). Comparative studies were adopted for the BoB region (Ts *et al*., 2020) utilizing two different models, the Regional Ocean Modelling System (ROMS) and the coupled Weather Research and Forecast (WRF). WRF is used to simulate

the oceanic and atmospheric conditions of the Bay. SST, SSS, sea level pressure, net heat flux, currents, and rising sea levels were compared between the simulation data and the original measurements. The findings revealed that the coupled model yielded superior accuracy in simulating the ocean. A study (Dandapat *et al*. 2021) revealed that the air-sea interface experiences a positive net flux which was the primary driver of the shoaling wave of the MLD during the Positive Indian Ocean Dipole (PIOD) year. This net flux had a greater impact on the shortwave radiation than the cooling effect of the latent heat flux. The resolution in the context of the BoB refers to the fineness of details used in computer-generated models or simulations to represent the physical processes and features of the BoB. Higher-resolution models can better capture small-scale features and processes. Forces in the BoB refer to external factors that change the energy levels in the atmospheric circulation and precipitation patterns in the area. Key atmospheric forces in the BoB include monsoon winds, temperature gradients between the land and the sea, and topographical features. Understanding the role of these atmospheric forces is important for improving the accuracy of weather prediction. A study on the BoB that focused on the circulation of the WBC and sea surface height anomaly (SSHA) using the ROMS and COADS was expanded as a Comprehensive Ocean-Atmosphere Data Set model for use in a climatological study (Wu *et al*., 2019). The study investigated the variations in the seasonal changeabilities of the ocean surface currents in the Eastern Indian Ocean throughout the pre-monsoon, summer monsoon, and post-monsoon periods, taking into account the impact of inconsistencies in the wind patterns between the Advanced Scatterometer (ASCAT) and QuikSCAT (QSCAT) data. (Srivastava *et al*., 2016; Thankaswamy *et al*., 2022). The study found that the wind variability was mostly confined to the upper 100 m portion of the water column and had a local effect. Additionally, the study emphasized caution when evaluating the wind-associated variables in ocean models (Sivareddy *et al*., 2015). This was constructed based on the observed data, and both experiments were compared to evaluate the seasonal variabilities in the temperature, salinity, and currents. (Lee *et al*., 2000; Sprintall, 2003; Yadav, 2022). They described the mixing of the top layer ranging from 30 – 100 m of the BoB in the seasonal cycle and was also observed using moored mixing meters. The extent of this salt flux was essential to determine the similarity of the model based on the salt budgets for the upper Bay of the region. (Cherian *et al*., 2020). Many studies have observed the inflection of Tropical Cyclone activity in the BoB and the influence of atmospheric and oceanic conditions (Ali *et al*., 2007; Chi, 2013; Goswami *et al*., 2003; Kikuchi *et al*., 2009; Lin *et al*., 2009) which stated that the present condition of the BoB was affected by climatological conditions. Climatological simulations are essential for assessing the circulation features by comprehensively representing the atmospheric processes, reproducing the historical climatic conditions, investigating circulation patterns, conducting sensitivity experiments, and projecting future climate scenarios. These simulations contribute to our understanding of climate dynamics and help in assessing the potential impacts of climate change on circulation patterns and associated weather and climate phenomena. The study aims to understand the upper ocean characteristics of BoB by analyzing the surface variables such as salinity and temperature using a high-resolution model simulation. This study was carried out in 2022 in India's BoB using the numerical model simulation.

## MATERIALS AND METHODS

### *Model, data, and methodology*

This study utilized the coastal and regional ocean community model (CROCO), a newly developed oceanic modeling system based on ROMS_AGRIF and SNH's non-hydrostatic kernel (testing of which is under process). The CROCO model is a free-surface, hydrostatic, primitive equation ocean model that incorporates algorithms from MARS3D (sediments) and HYCOM (vertical coordinates). It is a versatile modeling framework that combines physical, biogeochemical, and ecological processes to simulate and analyze the complex interactions within marine ecosystems. It is important to address the applicability, utility, and advantages of CROCO and its application in various fields, including coastal and ocean dynamics, marine ecology and ecosystems, coastal hazard and risk assessment, climate change, and sea-level rise. Its utility enhances our understanding of the complex interactions within coastal and regional ocean systems by simulating the physical, biogeochemical, and ecological processes.

Additionally, CROCO enables scenario prediction and analysis, data assimilation, and integrated assessments. The advantages of CROCO include high-resolution simulation, a flexible and modular framework, community collaboration, and multi-disciplinary integration. It was configured to cover the Bay of Bengal region (4˚N – 24˚N; 72˚E – 100˚E) with a horizontal grid resolution of approximately 10 km (256 × 249 grid points). The model used a stretched terrain-following S-coordinate system. Determination of the boundary conditions involved closed northern, eastern, and major parts of the western boundaries. In contrast, the southern boundary remained open, with temperature and salinity values relaxed to the Levitus monthly climatology. The model consisted of 32 vertical S-coordinate layers, and the bottom topography was derived from the Earth Topography Two-Minute digital terrain model (ETOPO2) data as shown in Fig. 1 and shows the geographic location of the area of study in the BoB, India. Significant attention should be provided to the distinctive bathymetric features of this region, as they potentially play a crucial role in governing deep circulation. This study was carried out in 2022 in the BoB region of India using the numerical model simulation.

*Data sources and evaluation methods*

The reanalysis datasets, along with the *in situ* data sets from Array for Real-time Geostrophic Oceanography (ARGO), World Ocean Atlas (WOA), Comprehensive Ocean-Atmosphere Data Set (COADS), and Hydro data, were utilized for evaluating the Simulation, Simple Ocean Data Assimilation (SODA) and Estimating the Circulation and Climate of the Ocean (ECCO), and conducting the comparisons between the models. The validation of the model involved the analysis of the correlation coefficient, root mean square difference, and standard deviation (SD) using the Taylor diagram to compare the different datasets and model simulations. The Taylor diagram serves as a comprehensive statistical tool that integrates these measures, aiding in the assessment of the predictability of the model.

*Experimental setup used for the simulation*

To understand the seasonal variability of the upper ocean in the BoB, climatological simulations were conducted for eight years using the CROCO Model. To ensure that the model accurately represented the real-world conditions, a 3-year spin-up period was allowed to adjust to the initial conditions and reach equilibrium. The comparisons made were based on simulations conducted over the next five years. Following the spin-up period, the model analyzed the time required for the evolution of kinetic energy during the 8-year model run, as shown in Fig. 2. The results obtained demonstrated that the volume-averaged kinetic energy gradually increased throughout the simulation, a particularly prominent increase during the monsoon. These were reliably consistent with previous studies highlighting the strong impact of monsoon winds on ocean circulation in the Bay.

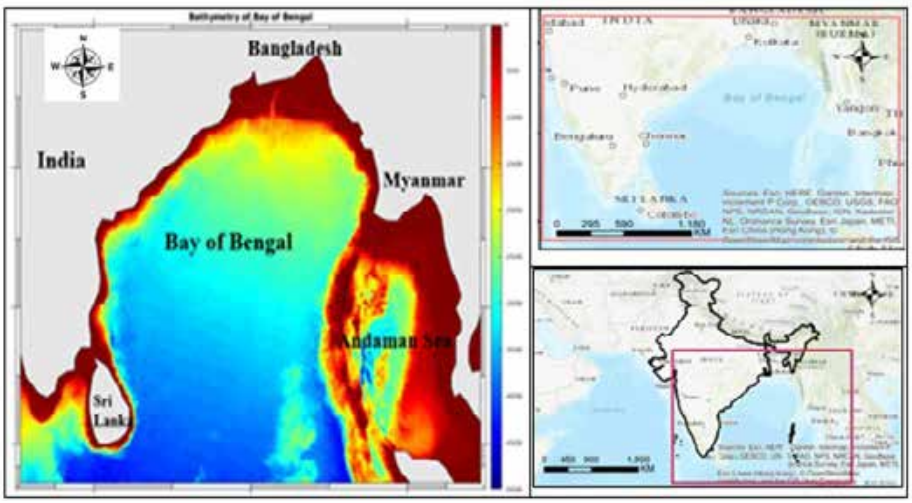


Fig. 1: Geographic location of the study area in the Bay of Bengal, India

These findings provide a valuable understanding of the complex dynamics of ocean drive in the BoB and highlight the importance of careful calibration and optimization of model spin-up periods accurately represent real-world circumstances. SST and SSS datasets from SODA and ECCO were utilized during the different seasons, including pre-monsoon, post-monsoon, monsoon, and winter. The model compared the statistical analysis of the ocean-atmospheric parameters like temperature and salinity. The bias was quantified as the disparity between the model outcomes and observed data. Using the model-based outputs, validating the results obtained with the Taylor diagram was then employed to estimate the correlation coefficient, root mean square deviation (RMSD), and standard deviation across the various datasets and model simulations. These statistical measures are integrated to evaluate the predictability of the model.

## RESULTS AND DISCUSSIONS

In this study, simulation was performed for the comprehensive validation using the CROCO model by comparing the simulation results with the observational data of various oceanic parameters. It evaluated the model's performance in determining the surface and sub-surface temperature and salinity. A validation analysis was conducted on a seasonal basis to ensure the comprehensive evaluation of the model's performance across different timescales. The results of the analysis indicated that the model performed well in capturing the observed changeabilities in the parameters studied.

*Simulation of seasonal variability in salinity*

Based on Fig. 3, the pre-monsoon simulations of surface salinity for the different datasets were analyzed. The ECCO reanalysis data showed that the northern bay had the lowest range of salinity distribution, ranging from 26 to 31 psu, while the eastern bay ranged from 31 to 34 psu. The southern and western bay had the highest temperature range of 33 to 35 psu, while the central bay had a one psu bias. The SODA dataset showed that the northern bay ranged from 26 to 31 psu, the eastern bay ranged from 31 to 33 psu, and the eastern bottom part ranged from 32 to 34 psu. The southern and western bay had the highest range of 33 to 35 psu. In the CROCO dataset, the north and eastern bay had the lowest distribution of salinity levels, ranging between 30 to 33 psu, while the southern and partially western bay had a higher distribution between 33 and 35 psu. The central bay had a salinity range of 32 to 33 psu, with a one psu bias. It is important to note that the temperatures in the eastern and western portions of the bay may be similar to those of the northern and southern parts, respectively. However, factors such as airflow and sea currents can cause temperature variations. In their study, Akhile *et al*. (2014) observed that during the pre-monsoon season, surface waters with salinity values below 31 were confined to the far northeastern region of the BoB. The winter salinity simulation and comparison with reanalysis data are presented in Fig. 4. The ECCO dataset demonstrated the least salinity near the northern, northeastern, and eastern parts of the region. The salinity in the northern bay extends from 28 to 32 psu while the eastern bay varies between 32 and 34 psu. In these regions, the simulation had a bias of one psu. The salinity was higher in the southern bay due to evaporation, ranging from 33 to 35 psu, and the salinity was higher on the southern coast of the western boundary. In the SODA data, the western coast recorded the lowest salinity ranging from 28 to 31 psu. The central bay had a high salinity ranging from 32 to 35 psu, while the open bay of the

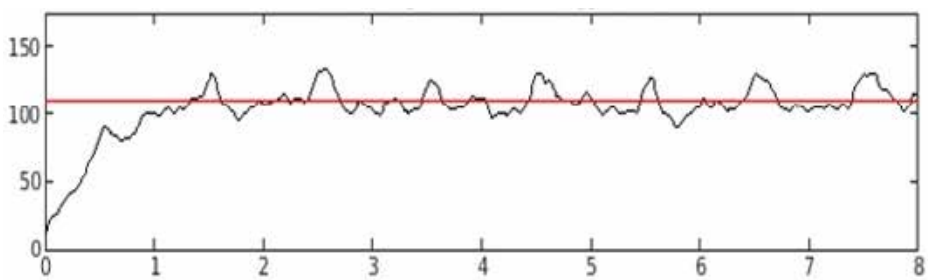


Fig. 2: CROCO 8 years average kinetic energy ($cm^2/s^2$)

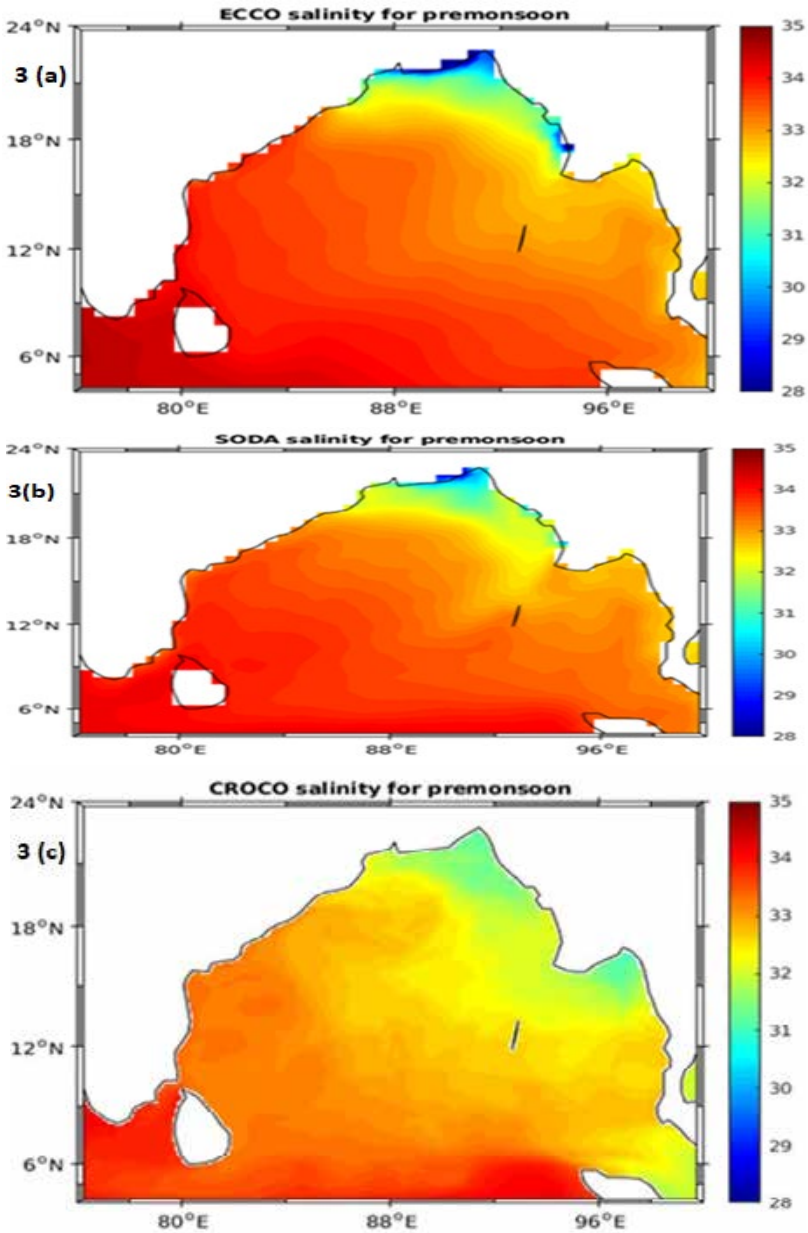


Fig. 3: Simulated salinity climatology plot for pre-monsoon (a) ECCO (b) SODA (c) CROCO

southern area had a high salinity distribution of 34 to 35 psu. The CROCO model simulation could predict better when compared to SODA and ECCO data. Additionally, depending on factors such as airflow and sea currents, the eastern and western parts of the bay had a similar salinity and temperature as in the northern and southern parts, respectively. This suggests an active role of horizontal advection on the southward migration of the SSS front. Salinity was less than in other seasons and ranged near the bay between 28 to 32 PSU, Akhil *et al*. 2014. In contradiction to expectations, the withdrawal of the fresh tongue takes place in December within the western region of BoB, roughly one month

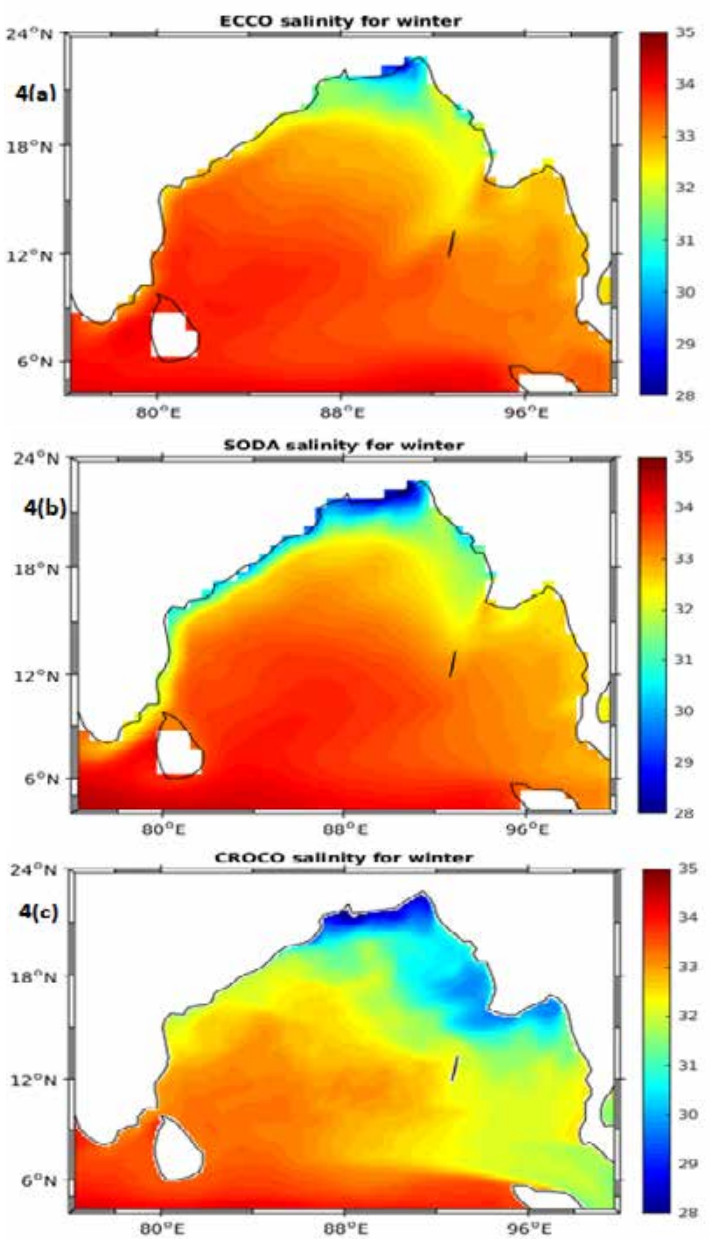


Fig. 4: Simulated salinity climatology plot for Winter (a) ECCO (b) SODA (c) CROCO

preceding the reversal of the prevailing current from equatorward to polewards. This observation implies that the advection process along the shore cannot be attributed to the driving force behind the northward retreat of the SSS front. Fig. 5 illustrates the salinity during the monsoon season. In the ECCO data, the lowest range of salinity distribution (28 – 31 psu) was located in the north, northeast, and northwest bay due to the influence of the southwest monsoon. The central bay had a salinity distribution of 32 to 34 psu. The south and southwest bays had the highest salinity of 34 to 35 psu, maintained by evaporation and ocean currents entering the bay. The geostrophic current plays a vital role in maintaining the mass

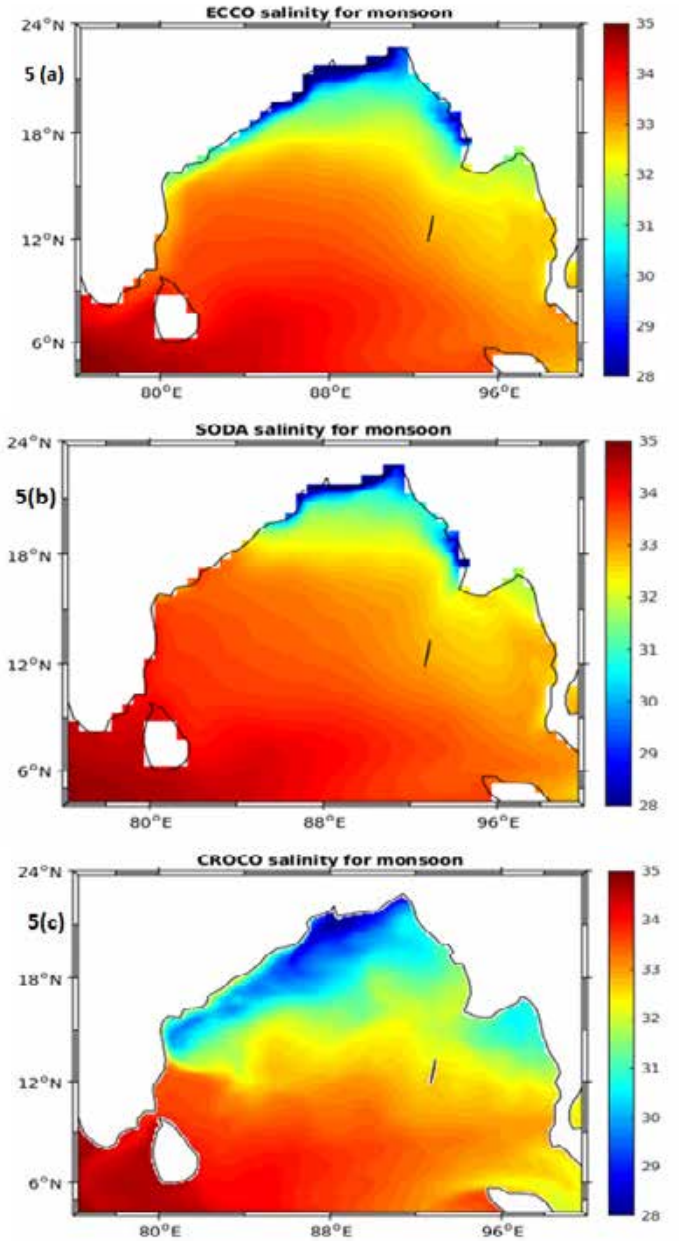


Fig. 5: Simulated salinity climatology plot for monsoon (a)ECCO (b) SODA (c) CROCO

level of low salinity water distribution that covers the bay, as detected from the circulation patterns in the surface salinity. Based on SODA data, it was found that the northern bay had the lowest salinity range of 28 to 31 psu, while the eastern bay had a bias of one psu, and the salinity level ranged between 32 and 33 psu. The south and southeast areas had high salinity due to ocean currents, and the range of values in all bay areas was the same as that in the ECCO data, with only a one psu bias. The western and partial southern regions (latitude 4° to 12° and longitude 74° to 88°) had a higher salinity range of 34 to 35 psu. Compared with the ECCO and SODA datasets, the model resulted in the same range of lowest salinity (28 to 31 psu) in

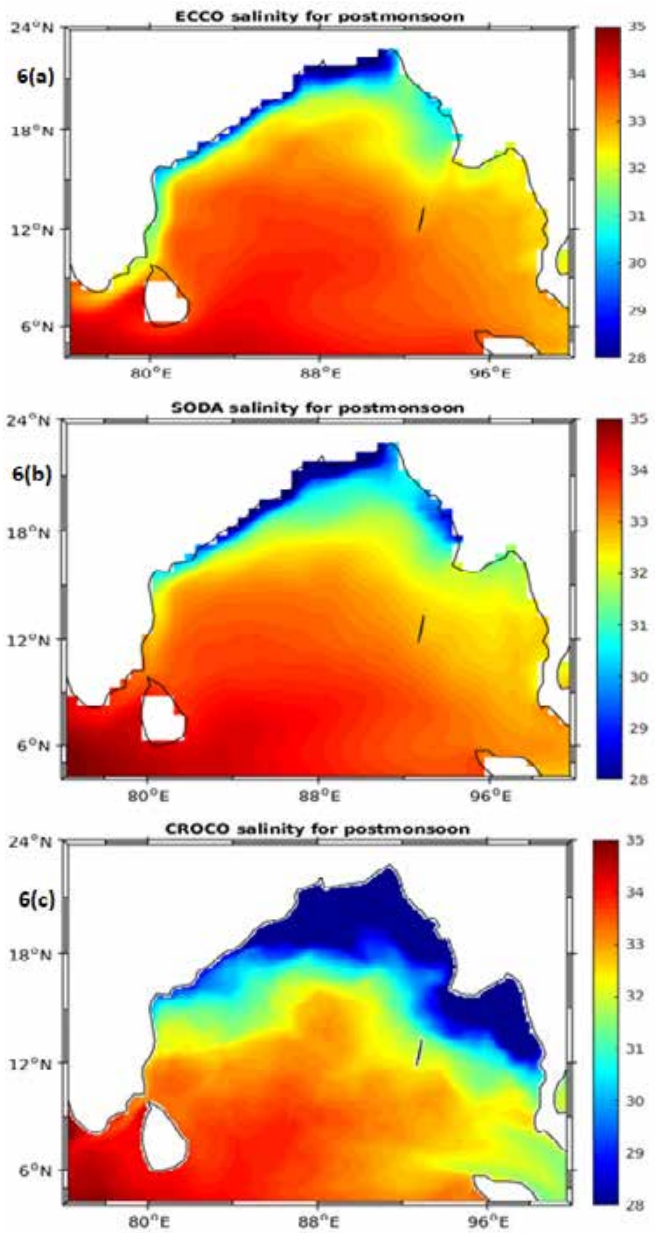


Fig. 6: Simulated salinity climatology plot for post-monsoon (a) ECCO (b) SODA (c) CROCO

the north to northwest regions. The central bay had a bias of one psu, while the east and southeast regions had low salinity due to the geostrophic current. The bottom-most bay opening near the south and west showed a high salinity (34 to 35 psu). The salinity levels in the bay can be affected by factors such as freshwater runoff from monsoon rains, tidal activity, and ocean currents. During monsoons, the surface salinity was low in the north and the western and eastern boundaries, about 15°N. This information was obtained from a previous study (Chakraborty and Gangopadhyay, 2016).

Fig. 6 presents the simulated salinity distribution in the Bay of Bengal. ECCO analysis showed that the

Table 1: Statistical statement for Salinity

| Data | Mean | SD | RMSD | Correlation |
|---|---|---|---|---|
| WOA | 32.4905 | 0.4604 | - | - |
| CROCO | 32.6370 | 0.3965 | 0.1338 | 0.9622 |
| ARGO | 33.0993 | 0.2495 | 0.3637 | 0.6179 |
| HYDRO | 33.0533 | 0.3470 | 0.3212 | 0.7174 |

Table 2: Statistical statement for Temperature

| Data | Mean | SD | RMSD | Correlation |
|---|---|---|---|---|
| WOA | 28.4886 | 0.8793 | - | - |
| CROCO | 28.9138 | 0.7001 | 0.2765 | 0.9640 |
| ARGO | 28.7416 | 0.8476 | 0.1307 | 0.9892 |
| COADS | 28.5491 | 0.8568 | 0.1750 | 0.9800 |

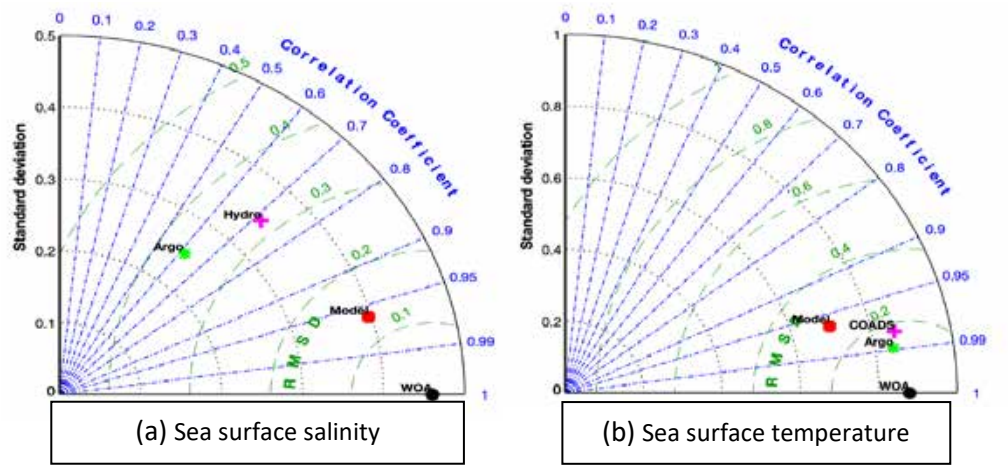


Fig. 7: Taylor Diagrams for CROCO model evaluation:
Correlation, RMSD, and standard deviation for (a) Sea surface salinity and (b) Sea surface temperature

lowest salinity ranges from 28 to 31 psu near the north and western parts of the bay, while the central and southern parts had the highest salinity, ranging between 33 to 35 psu. In the western boundary, the salinity varied from 31 to 33 psu. Similarly, SODA data analysis indicated that the lowest salinity, ranging from 28 to 31 psu, was found near the bay's north, east, and western boundary. Also, the southern bay possessed the highest salinity, ranging from 34 to 35 psu. The central bay showed a bias of one psu in the SODA data analysis. Freshwater runoff from the rivers in the post-monsoon season can lead to low salinity levels, while decreased input and increased evaporation during the post-monsoon season can result in high salinity levels. These changes in salinity levels can affect the local ecosystem and impact the distribution of marine life in the western part of the Bay region. The CROCO model predicted salt levels in the BoB, with the lowest salinity extending from 28 to 30 psu near the north and northeastern part of the bay. The western boundary had a medium range of salinity, ranging from 31 to 33 psu. The salinity ranged from 34 to 35 psu in the southern tip of the bay, which was the highest. The model satisfactorily predicted the salinity in all parts of the Bay, showing values to the ECCO and SODA datasets. In the study conducted by Akhile *et al.* 2014, it was observed that a region of low salinity (< 30 PSU) water formed

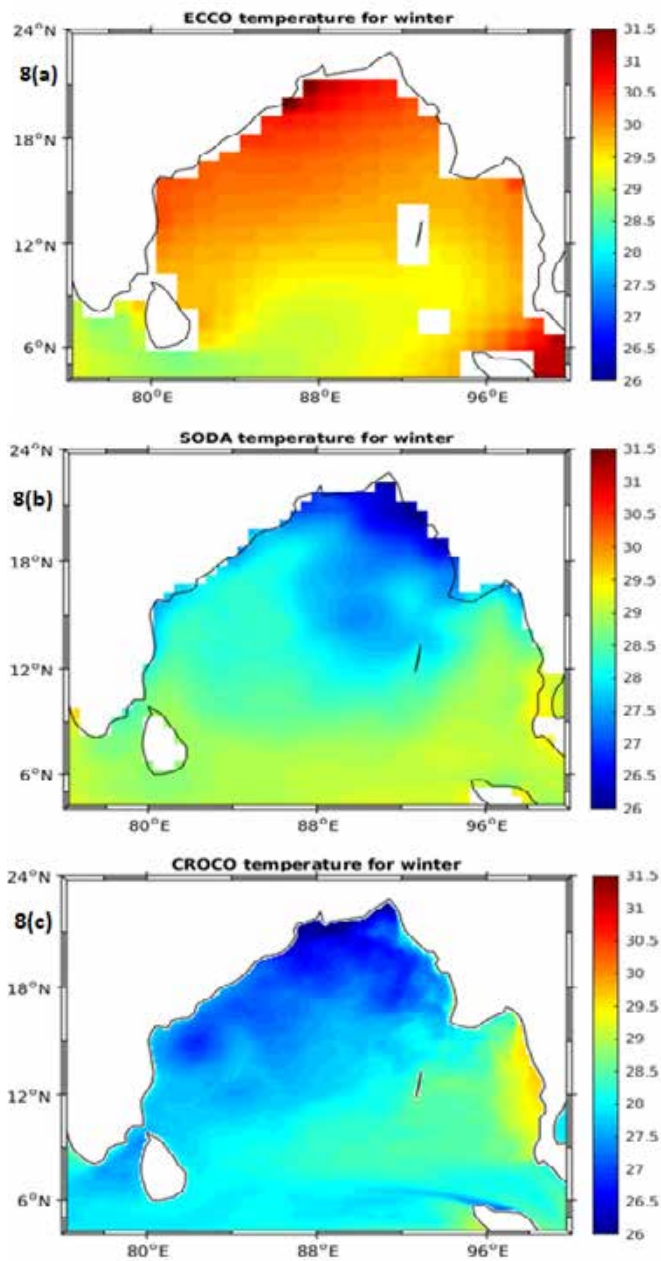


Fig. 8: Simulated temperature climatology plot for winter (a) ECCO (b) SODA (c) CROCO

in the northeastern BoB during August, September, and October. Evaluating the performance of a model often involves considering SSS as one of the main parameters, as shown in Fig 7(a). To validate the model, an analysis was conducted on the correlation coefficients, root mean square differences, and standard deviations using the Taylor diagram. This diagram enabled the comparison of different datasets and model simulations, functioning as a comprehensive statistical tool for assessing the model's predictability by integrating these measures. The available WOA, Hydro, and AGRO data were used to compare the series of monthly mean SSS values. The correlation coefficient values reveal that the

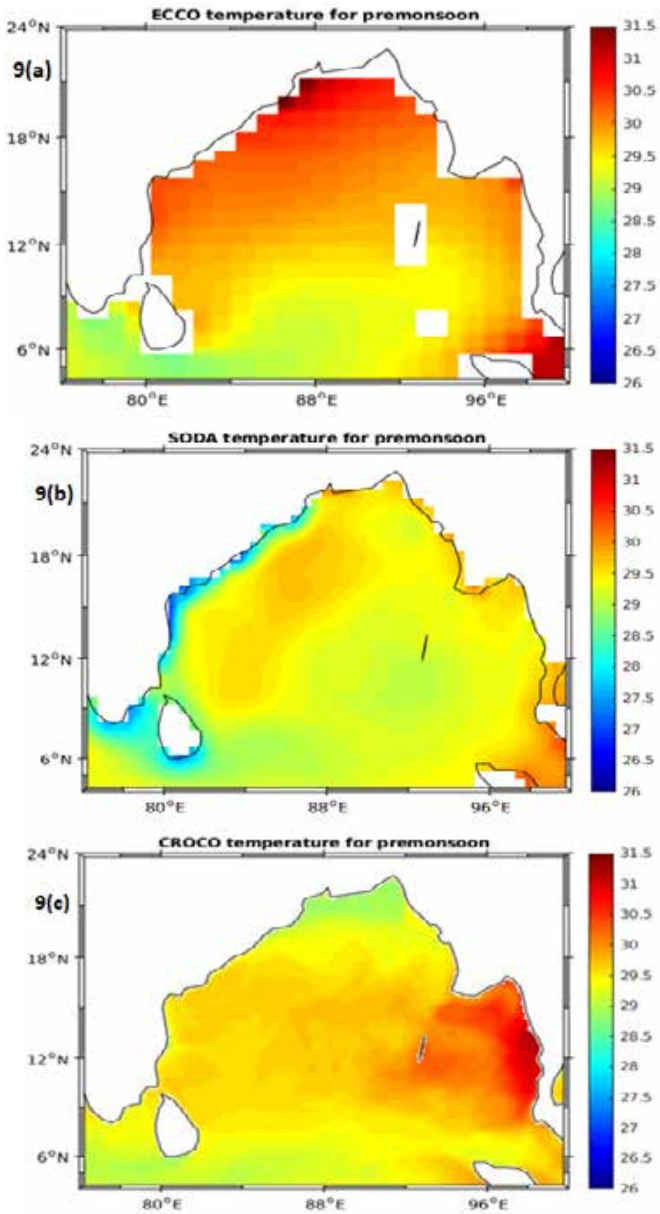


Fig. 9: Simulated Temperature climatology plot for pre-monsoon. (a)ECCO (b) SODA (c) CROCO

CROCO model exhibited a strong positive correlation (0.96) with the WOA dataset, which served as the standard for comparison. The correlation with the Hydro dataset was moderate (0.71), while the correlation with the AGRO dataset was comparatively weaker (0.61). These findings suggested that the CROCO model performed creditably in correlation with the WOA dataset but may show slightly lower performance with the Hydro and AGRO datasets concerning SSS. Based on the standard deviation values, it was observed that the CROCO model had the highest standard deviation (0.39) when compared to the WOA dataset, which was used as the base for the comparison. The standard deviation was slightly

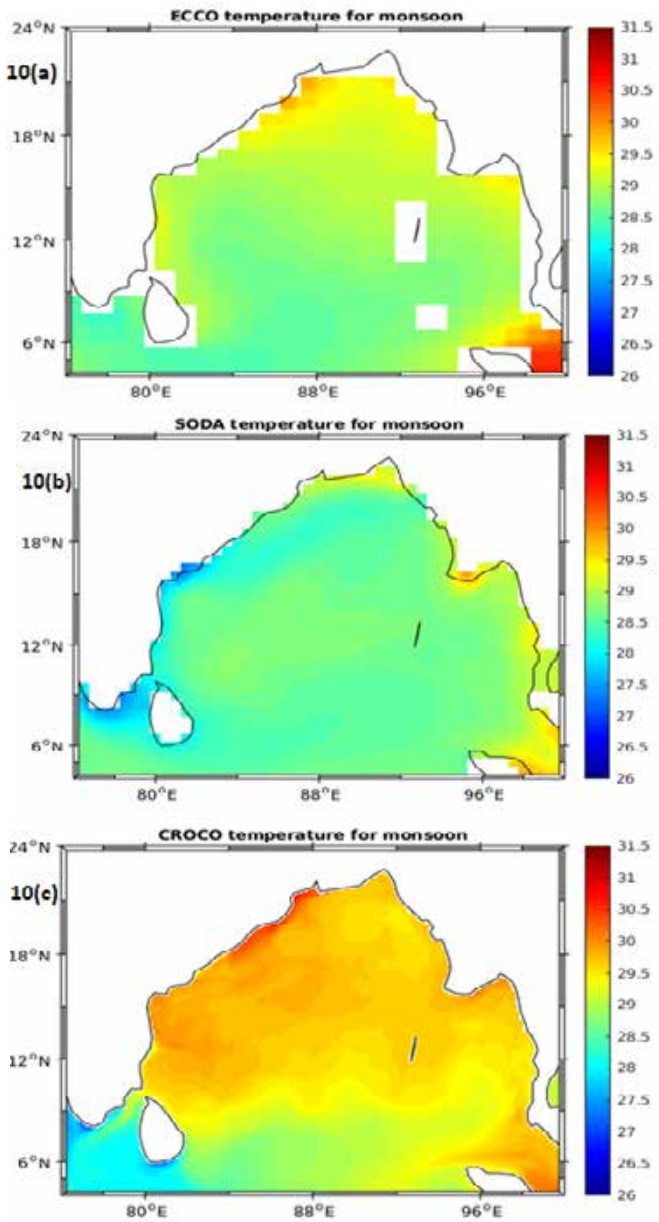


Fig. 10: Simulated Temperature climatology plot for monsoon. (a)ECCO (b) SODA (c) CROCO

lower for the Hydro dataset (0.34), and the lowest for the AGRO dataset (0.24). This suggested that the CROCO model had the highest prediction variability compared to the WOA, Hydro, and AGRO datasets. The CROCO model displayed a high strength when compared to the other datasets. Regarding the RMSD values, it can be observed that the CROCO model had the lowest RMSD value (0.13) when compared to the WOA dataset, which was used as the base for comparison. The RMSD was higher for the Hydro dataset (0.32) and the highest for the AGRO dataset (0.36). This suggested that the CROCO model had the best agreement with the WOA dataset regarding RMSD, indicating a lower overall deviation between

the model predictions and the WOA dataset values. Although, the Hydro and AGRO datasets showed higher RMSD values, suggesting potentially higher differences between the CROCO model-based predictions and these datasets. The surface salinity, as simulated by the coupled model, exhibited a correlation of 0.78 and a bias of 0.25 psu compared to the SODA values observed by Anandh *et al*. (2020). In comparison to the aforementioned model results, the current model demonstrated a significantly stronger correlation value of 0.96. The statistical statements for the salinity values are tabulated in Table 1.

*Seasonal variability simulation temperature*

Fig. 8 presented the simulation of temperature variations using the reanalysis of the ECCO and SODA datasets and the correlation with the CROCO model, for different seasons, including summer, winter, pre- and post-monsoon seasons. In winter, the ECCO dataset showed a temperature range of 26 ℃ – 31.5 °C with the north, east, and western regions of the bay having similar ranges and the southern bay having a lower range of 28.5 ℃ – 29.5 ℃. On the other hand, the SODA dataset showed lower temperatures of 26 ℃ – 27.5 ℃ in the northern and northeastern regions, with the western boundary having a slightly higher range of 28℃ – 29.5℃ and the south region had a range of 29 ℃ – 29.5 ℃. The analysis of the CROCO model showed that the temperature in the north and the northeastern boundaries ranged from 26 ℃ – 28 ℃, with the western boundary having a higher range of 27 ℃ – 28 ℃. Those of the central and southeastern ranged from 28 ℃ – 29.5 ℃, with a bias of 1 ℃, while that of the southern bay ranged from 27.5 ℃ – 28.5 ℃. During the winter, the prevailing winds from the northeast bring cool air from the land to the sea, which causes the temperature in the northern part of the Bay to be slightly lower than in the southern part. The WBC, which flows from the east to the west, influences the temperature in the BoB by bringing warm water from the equatorial region to the bay. This can raise the temperature in the western part of the bay, especially during the winter. Accordingly, the temperature varied conditionally based on the location and season and was influenced by the wind patterns and ocean currents in the BoB. Akhter *et al*. (2021) stated the winter temperature reached the highest value of 26 ℃ to 27.3 ℃, compared with other results; hence the model was predicted accurately.

According to Fig. 9, in the pre-monsoon season, the reanalysis of the ECCO dataset showed that the north, east, and western boundaries of the Bay demonstrated temperatures ranging from 30 ℃ to 31.5 ℃, while that of the southern boundary ranged from 28 ℃ to 29.5 ℃. These were typically observed between March and May. The northern part of the bay showed higher temperatures than the southern regions. Although, temperatures in the eastern part and western bay can vary depending on the airflow and sea currents. In the SODA analysis, the temperature near the boundary on the west side of the bay ranged from 26 ℃ to 28.5 ℃. Near the central bay was 28.5 ℃ to 29.5 ℃ and near the northeastern bay was 29 ℃ to 30 ℃. In the summer, the Bay experiences a north-northeast wind, which brings cool air from the land to the bay. Coastal upwelling also occurs during this season, causing colder water from the depths to rise to the surface due to winds blowing parallel to the coast and pushing surface water away from the shore. As per the results of the model analysis, the temperature in the north and southern bay ranged from 28.5 ℃ to 29 ℃, whereas, in the eastern bay, it varied from 30 ℃ to 31.5 ℃, Akhter *et al*. (2021). In spring, it reached 29.6 ℃, the highest value, and the western part of the bay ranged from 28.5 ℃ to 29.5 ℃. The bias in the central part was 1, and the temperature in all bay areas depends on the airflow and currents. The BoB is influenced by the equatorial counter-current, a warm ocean current that flows from west to east and can help warm the bay waters during the pre-monsoon season. According to Fig. 10, the ECCO dataset showed that in the northern bay, the temperature range was between 29.5 ℃ to 31 ℃, while the eastern, western, and southern bays ranged from 28 ℃ to 29 ℃. The central bay also recorded similar temperature ranges. These variations were influenced by the southwest monsoon, which brings moist and warm air starting from the Indian Ocean to the BoB region. The SODA dataset indicated that the northern and eastern bays had the highest temperature range, which was between 28 ℃ to 30.5 ℃, while the southern and central bays had a range of 28 ℃ to 29 ℃. The western bay had the lowest temperature range of 26 ℃ to 28.5 ℃. On the other hand, the CROCO model showed that the temperature range varied from 29 ℃ to 31.5 ℃ in all three bays, namely the northern,

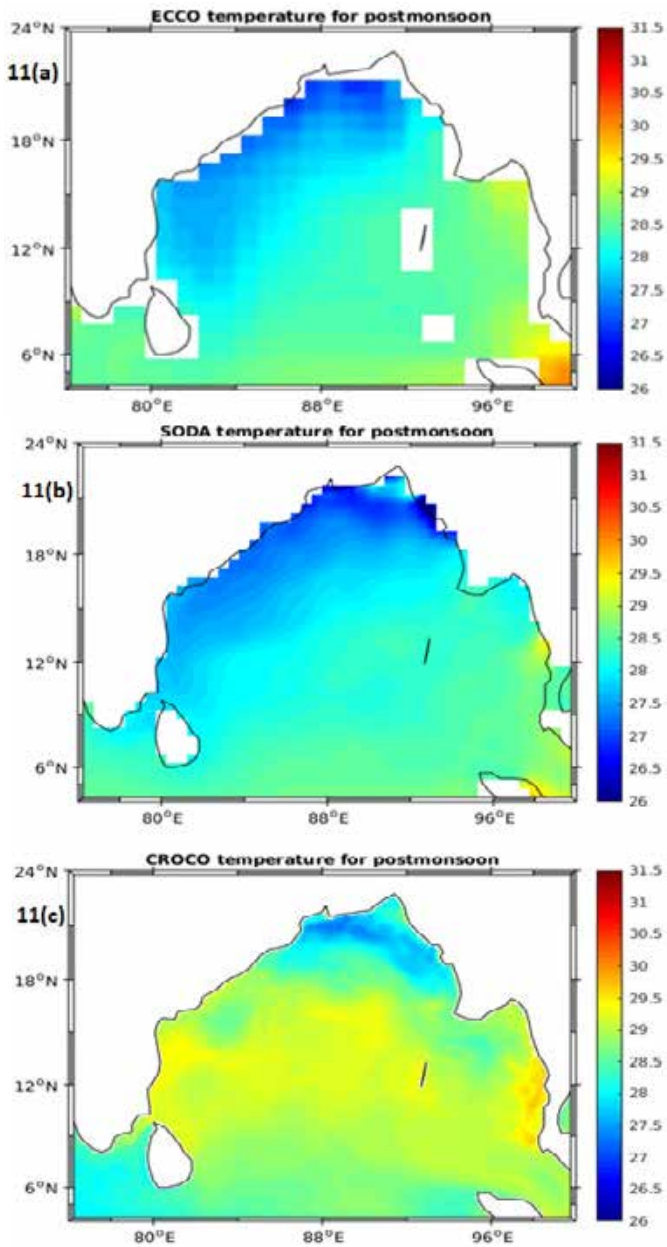


Fig. 11: Simulated Temperature climatology plot for post-monsoon (a) ECCO (b) SODA (c) CROCO

eastern, and southern bays. The central bay also had a maximum temperature range of 29 ℃ to 30 ℃. The tip of the western bay had a minimum temperature range of 27.5 ℃ to 28.5 ℃. It is worth noting that the monsoon winds and ocean currents also influence the wind patterns in the western bay in the BoB. Incidentally, EICC, which flows from east to west, can bring warm water from the equatorial region to the western side, raising the temperature and affecting the wind patterns. Monsoon seasons also affect the wind patterns in this area, bringing alternating winds from different directions throughout the year. In the eastern bay, wind patterns can vary depending on the location, but the monsoon winds generally influence

them. Throughout the northeast monsoon, winds can be cool and dry, while in the southwest monsoon, they are warm and moist. Overall, the temperature variations and wind patterns in the BoB can have significant implications for marine life, ecosystems, and climate. Additional research is required to comprehensively understand these factors impact on the region and their potential evolution over time. The simulated results from Fig. 11 for the post-monsoon season indicated that the ECCO dataset recorded the highest temperatures, extending from 29 ℃ to 30 ℃, in the eastern portion of the bay of the bottom-most bayline. Meanwhile, the central bay recorded a temperature range of 27 ℃ to 28.5 ℃, and the northern and western bays remained the coldest, with a range of 26 ℃ to 28 ℃. On the other hand, the SODA dataset records varying temperatures depending on the bay, ranging from 26 ℃ to 27 ℃ in the western bay, 27.5℃ to 28.5℃ in the eastern and southern bays, and 28 ℃ to 30 ℃ in the southern bay. Although, the central bay had a 1 ℃ bias. During the post-monsoon season, typically from October to December, the local weather conditions and ocean currents influence the temperature variations in the BoB. As the summer heat dissipates, the water temperature begins to cool, especially more quickly in the part of the northern bayside, leading in the direction of a north-south temperature gradient. The cyclonic activity typically increasing during this season can also impact the water temperature. The surface temperatures exhibited similarity in both simulations, except for a minor cooling effect observed during the summer, monsoon, and post-monsoon periods. The surface temperatures were around 28.9 ℃ throughout the year, as reported in a study conducted by Jana *et al*. (2015).

Validating the results obtained from the Taylor Diagram, Fig. 7(b), the CROCO model showed a strong positive linear relationship with the WOA, COADS, and AGRO data sets for the sea surface temperature, with correlation coefficients varying from 0.96 to 0.98. This suggested that the CROCO model was highly correlated with these data sets, particularly AGRO, indicating its potential accuracy in predicting the sea surface temperature. The standard deviation for the CROCO model compared with the WOA data set was 0.7, indicating that a relatively low level of variation occurred between the CROCO model and the WOA data set for sea surface temperature and the level of variation of the CROCO model when compared with the COADS data set was 0.85. This indicated a slightly higher variation or dispersion between the CROCO model and the COADS data set for sea surface temperature when compared to the WOA data set. The level of variation of the CROCO model compared with the AGRO data set was 0.84, indicating similar variations between the CROCO model and the AGRO data set for sea surface temperature compared to the COADS data set. The CROCO model exhibited an RMSD of 0.27 when compared to the WOA data set, signifying an average difference of 0.3. Similarly, when compared to the COADS data set, the CROCO model yields an RMSD of 0.27, indicating a smaller average difference. The CROCO model demonstrated an RMSD of 0.13 for the AGRO data set, suggesting a similar average difference of 0.1 compared to the COADS data set for the sea surface temperature RMSD was 0.17. Overall, the CROCO model displayed relatively smaller average differences when compared to the WOA, COADS, and AGRO data sets for sea surface temperature, as evident from the RMSD values obtained. Lower RMSD values indicated better agreement between the model and the data, with the COADS and AGRO data sets exhibiting slightly smaller average differences in comparison to the WOA data set. SST is captured well by the coupled model (the correlation coefficient was 0.96 compared to TRMM TMI), (Anand *et.al.*, 2020). Compared with the above results, the CROCO model correlated well with the temperature as the coefficient was 0.98. The statistical statements for the temperature values are tabulated in Table 2.

## CONCLUSIONS

The findings of this study reveal seasonal variations in temperature and salinity within the BoB region. During the winter and post-monsoon seasons, the southern area of the open bay exhibited a high salinity distribution ranging from 34 to 35 psu. The model used in this study accurately predicted the salinity values throughout the bay, aligning closely with the ECCO and SODA datasets. The salinity and temperature levels in the eastern and western parts of the bay resemble those in the northern and southern parts, respectively, and are influenced by factors such as airflow and sea currents. During the monsoon season, the geostrophic current played a vital role in maintaining the mass level of low

salinity water that covers the bay, as indicated by the observed surface salinity circulation patterns. Factors like freshwater runoff from monsoon rains, tidal activity, and ocean currents can impact salinity levels. The correlation coefficient values demonstrate a strong positive correlation (0.95) between the CROCO model and the WOA dataset, serving as a benchmark for comparison. This suggested that the CROCO model exhibited the closest agreement with the WOA dataset regarding RMSD, indicating minimal deviation between the model-derived predictions and the WOA dataset values. Although, the Hydro and AGRO datasets displayed higher RMSD values, suggesting potential differences between the CROCO model-based predictions and these datasets. Additionally, the analysis of the CROCO model highlighted a temperature range of 27 ℃ to 28 ℃ in the western boundary of the bay during winter. The WBC, which flows from the east to the west, influences the temperature in the BoB by transporting warm water from the equatorial region to the bay. This can elevate the temperature in the western part of the bay, particularly during the winter season. The model analysis indicates a temperature range of 30 ℃ – 31.5 ℃ in the eastern bay and 28.5 ℃ – 29.5 ℃ in the western part. The BoB is influenced by the EICC, a warm ocean current that flows from the west to the east and contributes to the warming of the bay waters during the pre-monsoon season. In the monsoon season, the CROCO model demonstrated a temperature range from 29℃ – 31.5℃ in all three bays: north, east, and south. The EICC, flowing from the east to the west, can bring warm water from the equatorial region to the western side, raising the temperature, and affecting wind patterns. During the northeast monsoon, winds tend to be cool and dry, while the southwest monsoon brings warm and moist winds. The temperature and wind pattern variations in the BoB significantly affect marine life, ecosystems, and climate. During the post-monsoon period (October to December), the water temperature starts to cool, especially in the North Bay, leading to a north-south temperature gradient. Local weather conditions and ocean currents influenced temperature fluctuations in the northern and eastern regions, as well as the southern and western sides. The presence of a counter-current played a significant role in warming the bay waters, particularly during the pre-monsoon period. Furthermore, as the summer heat dissipates, the water temperature decreases, with a pronounced cooling effect observed along the northern side of the bay during the post-monsoon phase. Lower RMSD values indicated a higher level of agreement between the model and the data, particularly considering the COADS and AGRO datasets. Existing data were all low resolution (WOA, HYDRO, COADS, ARGO, SODA, and ECCO) and have produced high-resolution data without much deviation from the standard. For validation, the Taylor diagram demonstrated that the model performed satisfactorily compared to the other datasets. The CROCO model exhibited a high correlation between temperature and salinity with a coefficient of 0.98. It is important to note that water salinity may also exhibit seasonal variations, requiring further studies to understand the extent and impact of these variations on the marine ecosystem.

## AUTHOR CONTRIBUTIONS

D. Jaishree reviewed the literature and contributed to the conceptualization, pre-processing, data analysis, preprocessing for simulations, and processing the model outputs and also prepared the manuscript text and edition. P.T. Ravichandran supervised the review work, was involved in the preparation of the manuscript, and reviewed the manuscript for publication.

## ACKNOWLEDGEMENT

Authors express gratitude to Dr. Deeptha Thattai, Dr. Arun Chakraborty (IITK) and Dr. Anandh for their guidance and for conducting scientific discussions which were instrumental in completing the research work.

## CONFLICT OF INTEREST

The author declares that there is no conflict of interests regarding the publication of this manuscript. In addition, the ethical issues, including plagiarism, informed consent, misconduct, data fabrication and/or falsification, double publication and/or submission, and redundancy have been completely observed by the authors.

## PUBLISHER'S NOTE



## ABBREVIATIONS

| | |
|---|---|
| *%* | Percent |
| *°C* | Degree Celsius |
| *$Cm/s^2$* | Centimeter per square second |
| *ASCAT* | Advanced scatterometer |
| *ARGO* | Array for real-time geostrophic oceanography |
| *BoB* | Bay of Bengal |
| *COADS* | Comprehensive ocean-atmosphere data set |
| *CROCO* | Coastal and regional ocean community model |
| *ECCO* | Estimating the circulation and climate of the ocean |
| *EICC* | East India Coastal Current |
| *ETOPO2* | Earth topography 2–minutes |
| *km* | Kilometer |
| *$Km^2$* | Square kilometer |
| *m* | Meter |
| *MLD* | Mixed layer depth |
| *PIOD* | Positive Indian ocean dipole |
| *Psu* | Practical salinity unit |
| *QSCAT* | QuikSCAT |
| *RMSD* | Root mean square deviation |
| *ROMS* | Regional ocean modelling system |
| *SODA* | Simulation, simple ocean data assimilation |
| *SSHA* | Sea surface height anomaly |
| *SSS* | Sea surface salinity |
| *SST* | Sea surface temperature |
| *$W/m^2$* | Watt per square meter |
| *WBC* | Western boundary current |
| *WOA* | World ocean atlas |
| *WRF* | Weather research and forecast |

## REFERENCES

Akhter, S.; Qiao, F.; Wu, K.; Yin, X.; Chowdhury, K.M.A.; Chowdhury, N.U.M.K., (2021). Seasonal and long-term sea-level variations and their forcing factors in the northern Bay of Bengal: A statistical analysis of temperature, salinity, wind stress curl, and regional climate index data. Dyn. Atmos. Oceans., 95: 1-23 (**23 Pages**).

Akhil, V.P.; Durand, F.; Lengaigne, M.; Jerome Vialard, J.; Keerthi, M.G.; Gopalakrishna, V.V.; Deltel, C.; Papa, F.; Ement De Boyer, C.; Egut, M., (2014). A modeling study of the processes of surface salinity seasonal cycle in the Bay of Bengal. J. Geophys. Res. C: Ocean. 119(6): 3926 – 3947 (**22 Pages**).

Ali, M.M.; Jagadeesh, P.S.V.; Jain, S., (2007). Effects of eddies on Bay of Bengal cyclone intensity. Eos, Trans. Am. Geophys. Union. 88(8): 93-104 (**12 Pages**).

Amsalia, N.; Haditiar, Y.; Wafdan, R.; Ikhwan, M.; Chaliluddin, M.A.; Sugianto, S.; Rizal, S., (2022). The currents, sea surface temperature, and salinity patterns in the Bay of Bengal. E3S Web of Conferences. 339 02001: 1–7 (**7 Pages**).

Anandh, T.S.; Das, B.K.; Kumar, B.; Kuttippurath, J.; Chakraborty, A., (2018). Analyses of the oceanic heat content during 1980–2014 and satellite-era cyclones over Bay of Bengal. Int. J. Climatol., 38(15): 5619 –5632 (**14 Pages**).

Anandh, T. S.; Das, B. K.; Kuttippurath, J.; and Chakraborty, A., (2020). A Comparative Analysis of the Bay of Bengal Ocean State Using Standalone and Coupled Numerical Models. Asia-Pac. J. Atmos. Sci., 57(2), 347–359. (**13 Pages**).

Chakraborty, A.; Gangopadhyay, A., (2016). Development of a high-resolution multiscale modeling and prediction system for Bay of Bengal, Part I: climatology-based simulations. Open J. Mar. Sci., 6: 145–176 (**32 Pages**).

Chi, N., (2013). The mixed layer salinity budget in the Central Equatorial Indian Ocean. J. Geophys. Res. C: Oceans., 1–18 (**18 Pages**).

Collins, M.; An, S.Il, Cai, W.; Ganachaud, A.; Guilyardi, E.; Jin, F.F.; Jochum, M.; Lengaigne, M.; Power, S.; Timmermann, A.; Vecchi, G.; and Wittenberg, A., (2010). The impact of global warming on the tropical Pacific Ocean and El Nĩo. Nat. Geosci., 3(6): 391–397 (**17 Pages**).

Cherian, D.A.; Shroyer, E.L.; Wijesekera, H.W.; Moum, J.N., (2020). The seasonal cycle of upper-ocean mixing at 8°N in the Bay of Bengal. J. Phys. Oceanogr., 50(2): 323–342 (**20 Pages**).

Dandapat, S.; Chakraborty, A.; Kuttippurath, J.; Bhagawati, C.; Sen, R., (2021). A numerical study on the role of atmospheric forcing on mixed layer depth variability in the Bay of Bengal using a regional ocean model. Ocean Dyn., 71: 963–979 (**17 Pages**).

Das, B.K.; Anandh, T.S.; Kuttippurath, J.; Chakraborty, A., (2019). Characteristics of the discontinuity of western boundary current

in the Bay of Bengal. J. Geophys. Res. C: Oceans. 124(7): 4464–4479 (**16 Pages**).

Dey, D.; Sil, S.; Jana, S.; Pramanik, S.; Pandey, P.C., (2017). An assessment of tropflux and NCEP air-sea fluxes on ROMS simulations over the Bay of Bengal region. Dyn. Atmos. Oceans., 80: 47–61 (**15 Pages**).

Dyn, C., (2010). The Indian summer monsoon pre-onset land surface processes and 'internal' interannual variabilities of the Indian summer monsoon. Clim. Dyn., 36: 2077–2089 (**13 Pages**).

Goswami, B.N.; Ajayamohan, R.S.; Xavier, P.K.; Sengupta, D., (2003). Clustering of synoptic activity by Indian summer monsoon intraseasonal oscillations. Geophys. Res. Lett., 30(8): 1-4 **(4 Pages)**.

Gao, Z.; Hu, Z.Z.; Zhu, J.; Yang, S.; Zhang, R.H.; Xiao, Z.; Jha, B., (2014). Variability of summer rainfall in Northeast China and its connection with spring rainfall variability in the Huang-Huai region and Indian Ocean SST. *J. Clim.*, *27*(18): 7086–7101 (**16 Pages**).

Gordon, A.L.; Mahadevan, A.; Hole, W.; Sengupta, D., (2016). Bay of Bengal: 2013 northeast monsoon upper-ocean circulation. Oceanography. 29(2): 82-91 (**10 Pages**).

Jana, S.; Gangopadhyay, A.; Chakraborty, A., (2015). Impact of seasonal river input on the Bay of Bengal simulation. Cont Shelf Res 104:45–62(**18 Pages**).

Jourdain, N.C.; Lengaigne, M.; Vialard, J.R.; Madec, G.; Menkes, C.E.; Vincent, E.M.; Jullien, S.; Barnier, B., (2013). Observation-based estimates of surface cooling inhibition by heavy rainfall under tropical cyclones. J. Phys. Oceanogr., 3(1): 1-17 (**17 Pages**).

Kikuchi, K.; Wang, B.; Fudeyasu, H., (2009). Genesis of tropical cyclone nargis revealed by multiple satellite observations. Geophys. Res. Lett., 36(6): 1–5 (**5 Pages**).

Lee, C.M.; Jones, B.H.; Brink, K.H.; Fischer, A.S., (2000). The upper-ocean response to monsoonal forcing in the Arabian Sea: seasonal and spatial variability. Deep Sea Res. Part II. 47(7-8): 1177–1226 (**50 Pages**).

Lin, I.I.; Chen, C.H.; Pun, I.F.; Liu, W.T.; Wu, C.C., (2009). Warm ocean anomaly, air sea fluxes, and the rapid intensification of tropical cyclone Nargis (2008). Geophys. Res. Lett., 36(3): 2–6 (**5 Pages**).

Levitus, S.; Antonov, J.I.; Boyer, T.P.; Baranova, O.K.; Garcia, H.E.; Locarnini, R.A.; Mishonov, A.V.; Reagan, J.R.; Seidov, D.; Yarosh, E.S.; Zweng, M.M., (2012). World ocean heat content and thermosteric sea level change (0-2000m), 1955-2010. *Geophysical Research Letters.*, *39*(10): 1–5 (**5 Pages**).

Liebmann, B.; Hendon, H.; Glick, D., (1994). The relationship and Indian between oceans tropical and the cyclones of the western oscillation pacific by brant liebmann cooperative institute for research in environmental sciences (CIRES), Campus Box 449, University of Colorado, Boulder, Colorado. J. Meteorolog. Soc. Jpn., 72(3): 401–411 (**11 Pages**).

Maneesha, K.; Ravichandran, M.; Yu, W., (2012). Upper ocean variability in the Bay of Bengal during the tropical cyclones Nargis and Laila. Prog. Oceanogr., 106: 49-61 (**13 Pages**).

Masumoto, Y.; Hase, H.; Kuroda, Y.; Matsuura, H.; Takeuchi, K., (2005). Intraseasonal variability in the upper layer currents observed in the eastern equatorial Indian Ocean. Geophys. Res. Lett., *32*(2): 1–4 (**4 Pages**).

Mahadevan, A. Hole, W.; Asaro, E.D., (2016). Variability of near-surface circulation and sea surface salinity observed from lagrangian drifters in the northern Bay of Bengal during the waning 2015 southwest monsoon. Oceanography. 29(2): 125-133 (**9 Pages**).

Rao, S.A.; Saha, S.K.; Pokhrel, S.; Sundar, D.; Dhakate, A.R.; Mahapatra, S.; Ali, S.; Chaudhari, H.S.; Shreeram, P.; Vasimalla, S.; Srikanth, A.S.; Suresh, R.R.V., (2011). Modulation of SST, SSS over northern Bay of Bengal on ISO time scale. J. Geophys. Res. C: Oceans., 116(9): 1-11 (**11 Pages)**.

Rao, S.A.; Behera, S.K., (2005). Subsurface influence on SST in the tropical Indian Ocean: Structure and interannual variability. Dyn. Atmos. Oceans., 39(1-2): (**11 Pages)**.

Roy Chowdhury, R.; Prasanna Kumar, S.; Chakraborty, A., (2021). Simultaneous occurrence of tropical cyclones in the northern Indian ocean: differential response and triggering mechanisms. Front. Mar. Sci., 8: 1-25 (**25 Pages**).

Schott, F.A.; McCreary, J.P., (2001). The monsoon circulation of the Indian Ocean. Prog. Oceanogr., 1(1): 1-123 (**123 Pages**).

Schott, F.A.; Xie, S.P.; McCreary, J.P., (2009). Indian ocean circulation and climate variability. Rev. Geophys., 47(1): 1–46 (**46 Pages**).

Sil, S.; Chakraborty, A., (2012). The mechanism of the 20°C isotherm depth oscillations for the Bay of Bengal, Mar. Geod., 35(3): 233–245 (**13 Pages**).

Sprintall, J., (2003). Seasonal to interannual upper-ocean variability in the drake passage. J. Mar. Res., 61(1): 27–57 (**31 Pages**).

Sivareddy, S.; Ravichandran, M.; Girishkumar, M.S.; Prasad, K.V.S.R., (2015). Assessing the impact of various wind forcing on INCOIS-GODAS simulated ocean currents in the equatorial Indian Ocean. Ocean Dyn., 65(9–10): 1235–1247 (**13 Pages**).

Srivastava, A.; Dwivedi, S.; Mishra, A.K., (2016). Intercomparison of high-resolution Bay of Bengal circulation models forced with different winds. Mar. Geod., 39(3–4): 271–289 (**19 Pages**).

Srivastava, A.; Dwivedi, S.; Mishra, A.K., (2018). Investigating the role of air-sea forcing on the variability of hydrography, circulation, and mixed layer depth in the Arabian Sea and Bay of Bengal. Oceanologia., 60(2): 169–186 (**18 Pages**).

Thankaswamy, A.; Xian, T.; Ma, Y.F.; Wang, L.P., (2022). Sensitivity to different reanalysis data on WRF dynamic downscaling for South China sea wind resource estimations. Atmosphere., 13(5), 1–23 (**23 Pages**).

Ts, A.; Das, B.K.; Kuttippurath, J.; Chakraborty, A., (2020). A coupled model analyses on the interaction between oceanic eddies and tropical cyclones over the Bay of Bengal. Ocean Dyn., 70: 327-337 (**11 Pages**).

Vinayachandran, P.N.; Satish Shetye, D.S.; Gadgil, S., (1996). Forcing mechanisms of the Bay of Bengal. Current Science., 71(10): 753–763 (**11 Pages**).

Vinayachandran, P.N.; Julian, J.P.M.; Hood, R.R.; Kohler, K.E., (2014). Numerical investigation of the phytoplankton bloom in the Bay of Bengal during northeast monsoon. J. Geophys. Res., 110(C12): 1-14 (**14 Pages**).

Webster, P.J.; Magaña, V.O.; Palmer, T.N.; Shukla, J.; Tomas, R.A.; Yanai, M.; Yasunari, T., (1998). Monsoons: processes, predictability, and the prospects for prediction. J. Geophys. Res. C: Oceans. 103(C7): 14451–14510 (**60 Pages**).

Wu, Z.; Jiang, C.; Deng, B.; Chen, J.; Long, Y.; Qu, K.; Liu, X., (2019). Numerical investigation of typhoon Kai-tak (1213) using a mesoscale coupled WRF-ROMS model. Ocean Eng., 175: 1–15 (**15 Pages**).

**AUTHOR (S) BIOSKETCHES**

**Jaishree, D.**, Ph.D. Candidate, Assistant Professor, Department of Civil Engineering, Faculty of Engineering and Technology, SRM Institute of Science and Technology, Kattankulathur - 603203, Chengalpattu District, Tamil Nadu, India.
- Email: *jaishred@srmist.edu.in*
- ORCID: 0000-0003-0401-068X
- Web of Science ResearcherID: NA
- Scopus Author ID: 57193997236
- Homepage: https://www.srmist.edu.in/faculty/jaishree-d-2/

**Ravichandran, P.T.,** Ph.D., Professor, Head of the Department of Civil Engineering, Faculty of Engineering and Technology, SRM Institute of Science and Technology, Kattankulathur - 603203, Chengalpattu District, Tamil Nadu, India.
- Email: *ravichap@srmist.edu.in*
- ORCID: 0000-0002-9555-2005
- Web of Science ResearcherID: NA
- Scopus Author ID: 23493524100
- Homepage: https://www.srmist.edu.in/faculty/dr-p-t-ravichandran/

**HOW TO CITE THIS ARTICLE**

*Jaishree, D.; Ravichandran, P.T., (2024). Exploring the upper ocean characteristics of a bay using coastal and regional ocean community model. Global J. Environ. Sci. Manage., 10(1): 1-20.*

**DOI:** 10.22035/gjesm.2024.01.***

**URL:** ***